Digital Object Identifier (DOI): 10.1109/TPEL.2017.2781258

IEEE Transactions on Power Electronics

A Quadruple Active Bridge Converter for the Storage Integration on the More Electric Aircraft

Giampaolo Buticchi
Levy Ferreira Costa
Davide Barater
Marco Liserre
Eugenio Dominguez

Suggested Citation

G. Buticchi, L. F. Costa, D. Barater, M. Liserre and E. Dominguez, "A Quadruple Active Bridge Converter for the Storage Integration on the More Electric Aircraft," in IEEE Transactions on Power Electronics, vol. PP, no. 99, pp. 1-1.

This article has been accepted for publication in a future issue of this journal, but has not been fully edited. Content may change prior to final publication. Citation information: DOI 10.1109/TPEL.2017.2781258, IEEE Transactions on Power Electronics

A Quadruple Active Bridge Converter for the Storage Integration on the More Electric Aircraft

Giampaolo Buticchi, *Senior Member IEEE*, Levy Costa, *Student Member IEEE*, Davide Barater, *Member, IEEE*, Marco Liserre, *Fellow, IEEE* and Eugenio Dominguez

***Abstract*—The More Electric Aircraft concepts aims at increasing the penetration of electric systems on the aircrafts. In this framework, the electrical power distribution system (EPDS) is of high importance. In order to improve the utilization of the generators and face the peak power demand without disconnecting the loads, different technologies of storage are employed. This paper proposes the use of a Quadruple Active Bridge converter, already employed in other fields, to interface a fuel cell, a battery and a supercapacitor bank to the DC bus of the EPDS. This objective can be achieved by employing multiple DC/DC converters, that allow an individual control of the energy sources and a good efficiency. Obtaining the same power control and efficiency with a multi-port power converter constitutes a challenge which is worth taking to reduce cost, volume and weight and increase the system reliability. A novel control based on PI controllers in conjunction with a decoupling system and current feed-forward allow shaping the power request to each port. This, however, leads to an asymmetrical loading of each port, which could decrease the efficiency. A laboratory prototype is used to confirm that this asymmetrical kind of operation, where each port processes a different amount of power, does not imply a marked reduction of efficiency.**

I. Introduction

The more-electric aircraft (MEA) concept is one of the major trends in modern aerospace engineering aiming at the reduction of the overall aircraft weight, operation cost and environmental impact. Electrical systems are employed to replace existing hydraulic, pneumatic and mechanical actuators, guaranteeing the same or higher reliability levels [1]. As a consequence, the on-board installed electrical power increases significantly and this challenges the design of the aircraft electrical power distribution systems (EPDS). The typical installed capacity of the electrical system on an existing medium-range aircraft increased from 100 kW of a Boeing 737 to more the 1 MW of the more recent Boing 787 [2]. To withstand the increase of energy request, the size of electrical generators is increased as well. However, the choice of the nominal power of new generators is still an open research theme. In fact, if the generators were designed to match the maximum peak power value requested during the different flight phases, the advantages of weight reduction and fuel saving would be probably lost [3]. In this scenario, the distribution retains a significant role as an intelligent power management could better exploit generation sources without necessarily increasing their rating. The immediate consequence of the above statement is to pose under discussion the conventional electrical power generation and distribution system. Under new trends of aircraft, the EPDS is designed on the concept of a highly decentralized, modular and flexible DC smart-grid, based on bi-directional DC/DC converters and solid state-based secondary distribution modules, with the utilization of energy storage systems. The parallel operation, along with power sharing capability of multiple generators, has been investigated to reduce generators size [4]. Nevertheless, the presence of power converters, often acting as constant power loads, introduces stability problem in the envisaged future EPDS [5], [6].

Apart the converters control strategies, the design of the best energy storage system still retains a key role in the electrification of aircraft. The correct dimensioning of the energy storage system has been investigated for some specific application [7] to identify the optimal trade-off between additional storage weight and fuel saving. A review of Emerging Energy Storage Solutions for Transportation was proposed in [8], focusing on different technologies of li-Ion batteries, fuel cells FC and ultracapacitors. These storage technologies have different properties, with regard to various attributes such as storage capacity, response time, power and cost. Therefore, it is impossible to specify a single energy storage solution that can satisfactorily fulfill the demands of a complex system such as an aircraft. The use of hybrid systems, adopting different technologies, is seen as the best solution for providing a better energy management and weight reduction for the MEA. One of the challenges in using hybrid energy systems is the development of interface electronics that allow an efficient exploitation of the different storage technologies. A straightforward way to interface multiple storage technology is to employ multiple DC/DC power converters, like Dual Active Bridge (DAB), connected to the same DC bus. This solution allows a good individual power control of the different sources and the efficiency of the power electronics can be optimized for each power source. However, it presents an increased number of control boards, communication links, high frequency transformer and power stages, decreasing the power density. Since all energy sources are coupled to the same DC bus, a multi-port solution would help making the system more power dense, reducing the overall number of

G. Buticchi is with Power Electronics, Machines and Control Group (PEMC), University of Nottingham Ningbo China, China, (e-mail: buticchi@ieee.org)

D. Barater is with University of Parma, Parma, Italy, (e-mail: davide.barater@unipr.it)

L. F. Costa and M. Liserre are with the Chair of Power Electronics, Christian-Albrechts University of Kiel, Kiel, Germany, (e-mail: zz, gdc, gibu, ml@tf.uni-kiel.de).

E. Dominguez is with SERTEC SL, Madrid (e-mail: eugenio.dominguez@sertec.net)

This article has been accepted for publication in a future issue of this journal, but has not been fully edited. Content may change prior to final publication. Citation information: DOI 10.1109/TPEL.2017.2781258, IEEE Transactions on Power Electronics

components. This paper proposes a Quadruple Active Bridge (QAB) that interfaces a hybrid storage system that include FC, battery and UCs, to the EPDS of future aircraft. The open challenges with respect to a multi DAB solution are the prioritization of the different energy sources depending on the frequency content of the bus request and the possible efficiency drop when the converter is operating in a very asymmetrical way, i.e., one storage port is providing most of the power.

The paper is organized as follows, Section II reviews the EPDS architectures, Sections III and IV describe the QAB converter and its control. Section V discusses the design of the QAB. Section VI and VII report the results. Simulations aim at showing different cases in a low-voltage scenario and will demonstrate the good power control capability of the proposed control. The experiments show a high-voltage demonstrator with efficiency measurement, reporting good results even in the case of asymmetrical operation. Finally, section VIII draws the conclusion.

II. Electrical Power Distribution System

Each aircraft manufacturer adopts different Electrical Power Distribution Systems with mixed AC and DC bus. A number of different voltage standards exist for the electrical system on large civilian aircraft:

- 28 V DC - low power loads/avionics on large aircraft and complete electrical system on small aircraft.
- 270 V DC (bipolar $\pm 135V$) - military aircrafts and some subsystems on some larger aircrafts.
- 115 V AC at 400 Hz - larger loads on large civilian aircrafts.
- 540 V DC (bipolar $\pm 270V$).
- 230 V AC at 400 Hz.

However, with MEA, the tendency is to replace traditional AC distribution and adopt only two main DC buses: a $\pm 270Vdc$ high voltage bus and a low 24 V dc bus mainly for avionics [2]. The AC sources are interfaced to the bus with AC/DC converters, the same for AC loads, such as electromechanical actuators, driven by DC/AC electric drives. This can increase efficiency, reduce weight and remove the need for reactive power compensation devices [9].

An example of EPDS for future regional aircrafts is shown in Fig. 1 where two main power generators and an auxiliary generator are connected to three independent bus bar that can work independently or connected together to enable power sharing between the generators. The system can also decide to exclude one bus bar in case of fault, reallocating the power between the generators. The low voltage buses include energy storage systems and in the scheme bidirectional DC/DC converters are used to exchange power between the High Voltage and Low Voltage buses. A Centralized Control Unit (CCU) synthesizes the best control strategy to manage the energy flow and supervise the functionalities of the DC/DC converters, deciding on-fly their operation in buck or boost mode.

During normal operation, the DC/DC converters are used in buck mode, charging the energy storage system if needed, but in case of emergency they can be used to supply critical high voltage loads. The choice of the best storage system is still under research, as fuel cells or battery are envisaged for their high energy density, whereas ultra/super capacitors can be included with the role of energy buffers, to help during high transient energy requests from electro mechanical actuators or other critical loads. However, the use of different kinds of storage poses issue that must be addressed by the EPDS. In fact, supercapacitors, batteries and/or fuel cells have different response times and an energy management system should feature a multi-scheme storage system, where depending on the optimization criteria (fuel consumption, life cycle maximization, stress of each component) different control schemes are activated.

As shown in the Ragone plot of Fig. 2, different storage technologies have different characteristics that, in relation to their specific energy (Wh/kg) and specif power (W/kg), make them more or less appealing for the different applications in grid distribution or transportation. The use of an hybrid system allows to cope with the different needs containing cost, weight and volume.

Because of the reduced number of conversion stages and the intrinsically DC characteristics of the storage, this paper focuses on the DC solution for 270 V / 28 V EPDS. The technical challenges of this design are to guarantee a precise and fast control of the power processed by the different sources while still guaranteeing high efficiency, power density and galvanic isolation for safety purpose.

III. The Quadruple Active Bridge Converter

A multiple port converter based on active bridges was proposed in 2007 in [10]–[12] as a solution to interface multiple sources and still retain the galvanic isolation. The converter retains the basic characteristics regarding power transfer and soft switching as the Dual Active Bridge converter.

The schematic of the QAB if presented in Fig. 5. The adopted control is the phase-shift control, that implies that each full-bridge is driven with a 50% duty cycle and the shifting between the voltage square waves determines the power transfer.

Fig. 4 shows the phase-shift modulation (a) and the possible models of the high-frequency transformer. The tightly coupled structure can be represented by a star equivalent (b) or delta equivalent (c). A modification in the phase-shift of one port affects the power transfer of all other ports. By using the delta model, the current that flows through the inductors depends only on the voltage sources connected at the inductor terminals. This means that it is possible to calculate the current, and as a consequence the power flow, like it is done for the DAB converter. By repeating this procedure for all the inductors connected at a specific node, the total power processed by a port can be evaluated.

Equation (1) describes the overall power that is processed by a single port, where n_{ij} is the turn ratio between the two ports, L_{ij} is the equivalent inductance from the two ports and d_{ij} is the phase shift angle normalized to 2π.

$$P_i = \sum_{j \neq i} \frac{n_{ij} V_i V_j}{L_{ij} f_{sw}} d_{ij} \left(1 - 2d_{ij}\right) \tag{1}$$

This article has been accepted for publication in a future issue of this journal, but has not been fully edited. Content may change prior to final publication. Citation information: DOI 10.1109/TPEL.2017.2781258, IEEE Transactions on Power Electronics

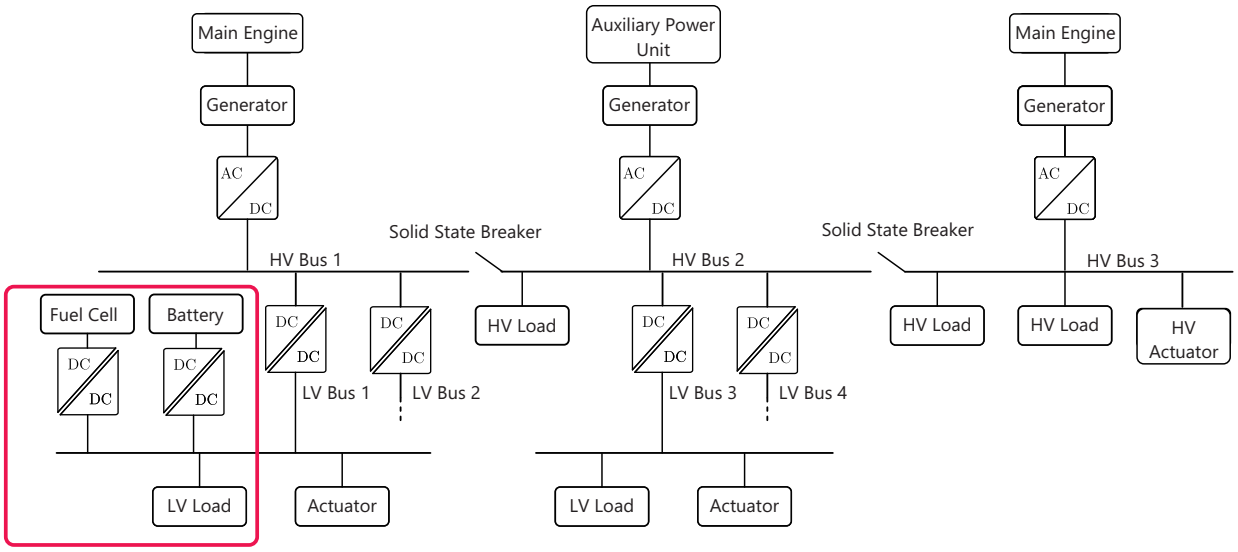

Fig. 1: Example of an electrical power distribution systems with the storage part highlighted.

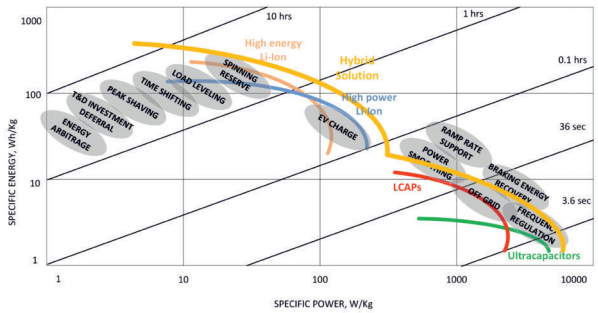

Fig. 2: Comparison of different storage systems characteristics in terms of specific energy and power

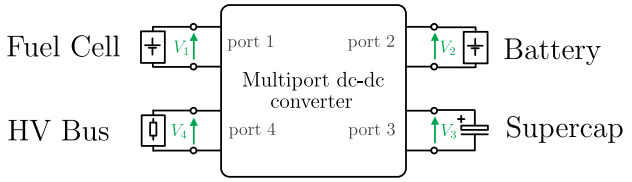

Fig. 3: Quadruple Active Bridge as a storage integration node connected to a DC bus.

One of the challenges of the QAB is that the individual control of the single ports, because a modification of one phase-shift would lead to unbalancing the power processed by all other ports. In order to prevent this behavior, a decoupling mechanism must be implemented. The first step is to perform a linearization of equation (1), assuming that the inductance are designed to have the converter operating for small phase shift.

Linearizing the equations around the zero phase shift leads to the matrix A of equation (2), where it is seen that variation in the voltage (because of oscillations in the supercapacitors voltage or in the DC bus) and differences in the inductance must be taken into account for a proper compensation. Inverting the matrix and normalizing it to the nominal values of the inductance and voltage levels allows decoupling the power flow.

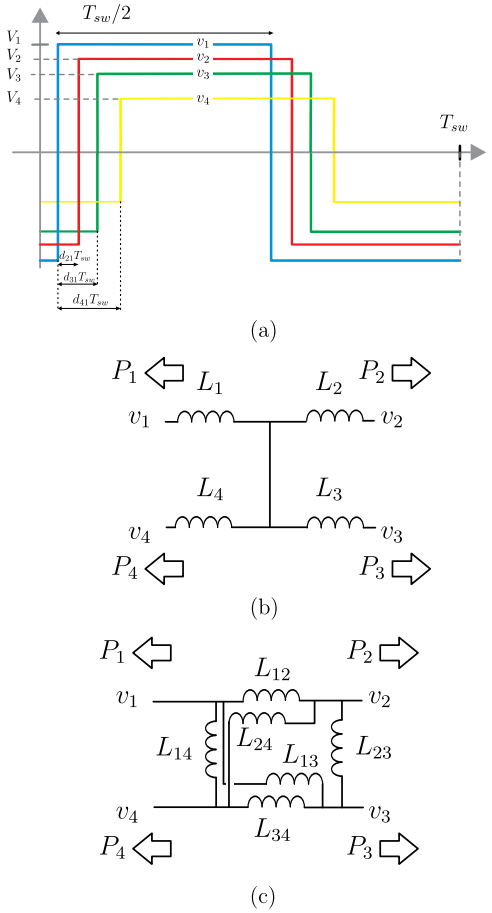

Fig. 4: QAB model. Phase-shift modulation (a), star model (b) and delta model (c).

This article has been accepted for publication in a future issue of this journal, but has not been fully edited. Content may change prior to final publication. Citation information: DOI 10.1109/TPEL.2017.2781258, IEEE Transactions on Power Electronics

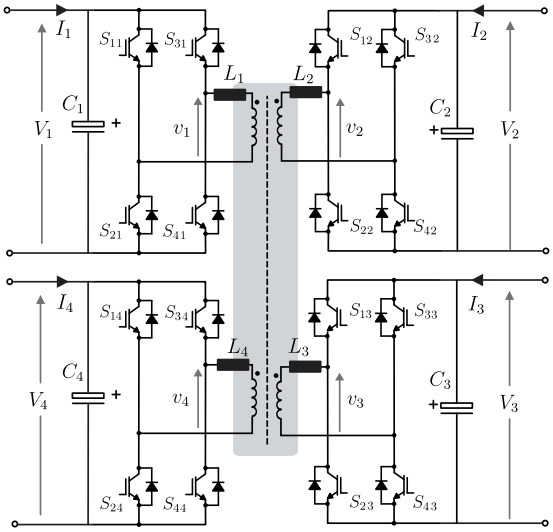

Fig. 5: Quadruple Active Bridge schematic.

IV. Control description and tuning

The objective of the control is to ensure a stable bus regulation, prioritizing the fast storage during the transient and keeping the fuel cell power level as constant as possible. Fig. 6 shows the control, where a combination of High-Pass-Filter (HPF) and Low-Pass-Filter (LPF) allows selecting the different frequency components that are processed by each port. In addition, a current control for the battery should be implemented to control the state-of-charge (SOC) and a DC Link control for the average voltage of the supercapacitor.

The decoupling block can be implemented by inverting the matrix A in equation (2) and normalizing, like shown in equation (3).

$$\begin{pmatrix} d_{41} \\ d_{42} \\ d_{43} \end{pmatrix} = \frac{V_n}{L_{lk}} A^{-1} \begin{pmatrix} d_{fuelcell} \\ d_{batt} \\ d_{supercap} \end{pmatrix} \tag{3}$$

In order to study the control, a simplified model is shown in Fig. 7. The assumption is that, after the decoupling, the power flow of each port can be realized independently, as if the converter was composed of three separate DAB, whose phase shift controls the power exchange. The model is realized on an equivalent DAB with equal voltages at primary and secondary sides V_n, with a frequency f_{sw} and leakage inductance L_{lk}. In these conditions, $K_{eq} = 4\frac{V_n}{f_{sw} L_{lk}}$. The output of the voltage control regulator is d_{DC}, that is then divided into the high- and low-frequency components for the different sources. The load current is modeled as a voltage dependent generator, that can represent a resistor R_{load} or other loads, depending on the equipment (constant impedance, constant current, constant power).

For the initial controller tuning, only the capacitor equation is considered, and a PI controller is tuned to achieve a target crossover frequency with the maximization of the phase margin [13]. For the bus voltage control, a crossover frequency of 300 Hz is selected, while for the supercapacitor voltage control only 1 Hz is chosen. In fact, it is important the voltage control of the capacitor does not affect the system. Overvoltage or undervoltage of the capacitor can be prevented by saturating the phase shift.

The control realized with a simple PI regulator has a main drawback: the higher the phase margin of the design, the higher the output impedance becomes. As a consequence, fast-changing load will deteriorate the voltage regulation unless a very fast controller is realized. Moreover, the output of the PI regulator is limited by the chosen bandwidth, making impossible for the supercapacitor to follow rapid power variations. For this reason, a current feed forward is used to reduce the output impedance and bypass the PI regulator during fast load variations, as shown in Fig. 6. The same objective could have been realized by applying an impedance shaping technique, like in [14].

Fig. 8 shows the frequency responses of the voltage control and of the output impedance with the voltage control and with the current feed-forward. As can be seen, the current feed-forward allows for a better disturbance rejection. Nominal voltages of 28 V for all ports, switching frequency f_{sw} = 20 kHz, bus capacitance 0.5 mF and L_{lk} = 1 uH.

V. QAB Converter Design

The proposed energy storage system aims at supplying a bus with a variable power consumption. A typical operation is sketched in Fig. 9, where the bulk power is provided by the fuel cell and the peak power is provided by the supercapacitors. The battery compensates for this difference. From the point of view of the design, this means that the port connected to the bus must have greater power processing capability than the other. Such a storage system can effectively realize the peak shaving, avoiding the overdesign.

In the following, it will be assumed that each storage port has the same maximum power capability, this means that the storage system will be able to supply for a short period three times the bulk power rating. The design procedure is described in Fig. 10.

Regarding the voltage design for the QAB, there are several possibilities. Considering the MIL-STD-704F standard, 270 V or 28 V buses are present. The first choice is to select if the energy storage system is connected to the HV or to the LV bus. For smaller aircrafts, it is sensible to choose a LV connection, due to the limited power requirements. This choice allows for an easier design of the energy storage, since fuel cells, batteries and supercapacitors are normally found for low voltage. The LV design will be shown in the simulation section.

If higher power is required, a HV design would be preferable, and the QAB can be connected to the HV bus. Although the storage voltage can still be in the LV range, this choice would imply a higher conversion ratio (i.e., more challenging transformer design). Moreover, higher current in the LV side and the usage of Silicon devices would deteriorate the system efficiency. For this reason, a symmetrical HV QAB can be designed for high power applications. The downside is that series connection of battery cells and supercapacitors would make the storage design more challenging. In fact, more complex balancing circuits to ensure the proper sharing of

This article has been accepted for publication in a future issue of this journal, but has not been fully edited. Content may change prior to final publication. Citation information: DOI 10.1109/TPEL.2017.2781258, IEEE Transactions on Power Electronics

$$\begin{pmatrix} P_1 \frac{f_{sw}}{n_1 V_1} \\ P_2 \frac{f_{sw}}{n_2 V_2} \\ P_3 \frac{f_{sw}}{n_3 V_3} \end{pmatrix} = \begin{pmatrix} \frac{V_4}{L_{14}} + \frac{V_2}{n_2 L_{12}} + \frac{V_3}{n_3 L_{13}} & -\frac{V_2}{n_2 L_{12}} & -\frac{V_3}{n_3 L_{13}} \\ -\frac{V_1}{n_1 L_{21}} & \frac{V_4}{L_{24}} + \frac{V_1}{n_1 L_{21}} + \frac{V_3}{n_3 L_{23}} & -\frac{V_3}{n_3 L_{23}} \\ -\frac{V_1}{n_1 L_{31}} & -\frac{V_2}{n_2 L_{32}} & \frac{V_4}{L_{34}} + \frac{V_1}{n_1 L_{31}} + \frac{V_2}{n_2 L_{32}} \end{pmatrix} \begin{pmatrix} d_{41} \\ d_{42} \\ d_{43} \end{pmatrix} = A\,[d] \qquad (2)$$

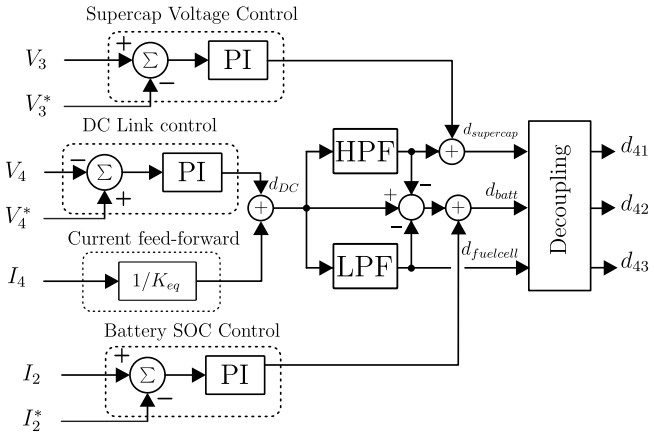

Fig. 6: Control of the QAB, including state-of-charge for the battery and voltage control for the supercapacitor.

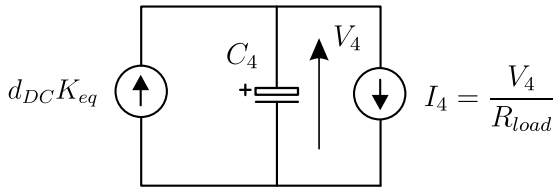

Fig. 7: Simplified model for the voltage control of the DC bus.

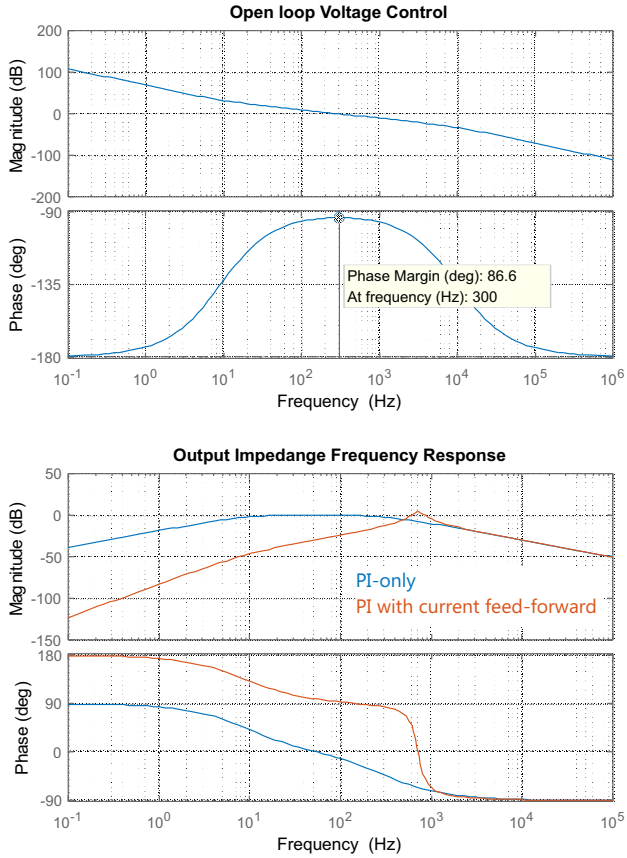

Fig. 8: Frequency response of the voltage control and of the output impedance.

the voltage among different cells would be necessary. The use of higher voltage would allow for SiC devices, that exhibit excellent on-state characteristic, increasing the system efficiency.

The main equations regarding the design are reported in Appendix I. After selecting the nominal power of the bus side, the equivalent needed inductance must be evaluated, equations (4)-(5). Equation (6) gives the peak value of the bus current, that can be used to calculate the current stress on all semiconductors, see Table III. As a simplification, the hypothesis of equal voltages and an unity ratio transformer is made. If different voltages are used, the parameters can be easily adapted by altering the turn ratio of the transformer and adapting the inductance following the square of the turn ratio rule.

The conduction losses, under the assumption of using MOSFETs, are calculated by (7), where the on-resistance ($R_{ds(on)}$) is function of the drain-source current (i_{ds}), junction temperature (T_J) and gate voltage (V_{gs}). Assuming a constant junction temperature and gate voltage, the equation is simplified to (8). The switching losses can be generally calculated by (9), where $N_{sw(on)}$ and $N_{sw(off)}$ are the number of turn-on and turn-off commutations, respectively, during the time interval T_{sw}. R_g is the gate resistance. It is assumed that the converter switches always with a constant voltage, a constant junction temperature, V_{gs} and R_g. Because of the ZVS operation, the turn-on losses are neglected, and a simplified equation can be written as presented in (10). The current in the output capacitance depends on the phase shift and on the output current, and is described in (11). An algorithm can be implemented to assist the high-frequency transformer design and calculate its losses. In this algorithm, the basic design is performed according to [15], where the number of turns is calculated, wires are selected and so on. To avoid the skin effect, litz wire is used. Then, only the DC losses on the wires are considered and it is calculated by (12). For the core losses, the generalized Steinmetz equation [16] is used, as presented in (13) and (14).

VI. Simulations

As aforementioned, simulations focus on a LV design with the goal of proving the effectiveness of the decoupling and feed-forward to achieve a precise individual power control. For each port, the voltage is 28 V and the rated current for the bus port is 90 A, this implies a total power of 2.5 kW. The rated normalized phase shift d_n is chosen equal to 0.1 (equivalent to

This article has been accepted for publication in a future issue of this journal, but has not been fully edited. Content may change prior to final publication. Citation information: DOI 10.1109/TPEL.2017.2781258, IEEE Transactions on Power Electronics

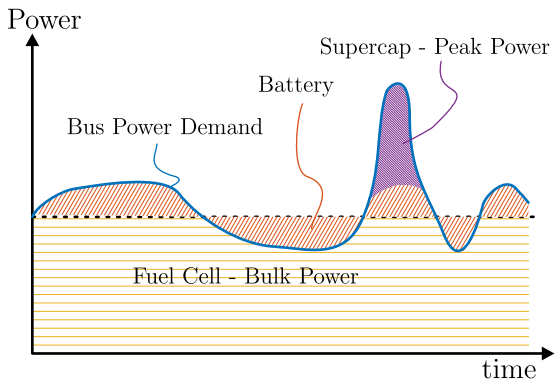

Fig. 9: Example of the power sharing targets between the different ports.

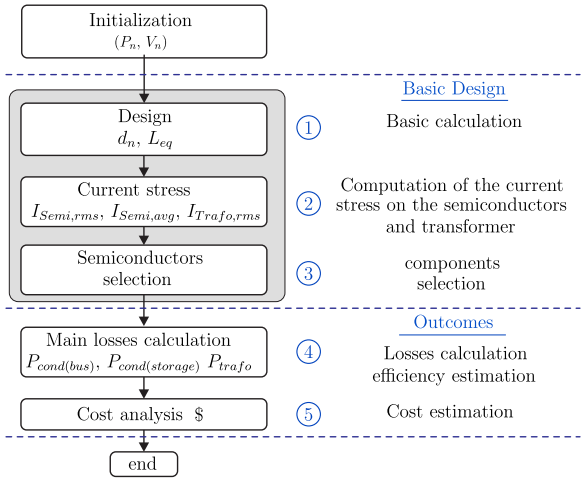

Fig. 10: Flowchart of the design for the QAB.

36 degrees), in order to have some control margin and to limit the reactive current between the ports [17]. Following equation (5), L_{eq} = 1.25 uH results. When the QAB is operating at full power, i.e., all storage ports transfer the rated power to the bus, the three ports operate in parallel. Following the star model of Fig. 4b, if all inductances are equal with a value L_{lk}, the overall equivalent inductance is $L_{eq} = 4L_{lk}/3$, this would result in a leakage inductance of 0.94 uH for each port. This value is chosen to be 1 uH in the simulations. Because the operation of the converter is intrinsically asymmetrical, i.e., the preferred power transfer direction is between the storage ports and the bus ports, a different mix of inductors can be chosen to reach the same equivalent inductor. In fact, the bus port could have a smaller inductor value than the other ports. This may be beneficial for optimization purpose, in fact the inductor connected to the bus port carries more current than the other. The design margin for the phase shift allows handing eventual design mismatches. A value of 500 uF is chosen for the output capacitance of each port. Table I summarizes the parameters of the simulations.

In the following several cases are reported, showing different transients. In all of them, the battery current reference is set to 3 A. The capacitance of the supercapacitors is 10 mF in this example. A purposely small value for the supercapacitor is

V_n (V_1, V_2, V_3, V_4)	28 V
P_n	2.5 kW
L_{lk} (L_1, L_2, L_3, L_4)	1 uH
L_{eq}	1.25 uH
C_1, C_2, C_3, C_4	0.5 mF
$C_{supercap}$	10 mF
$f_{3dB-bus}$	300 Hz
$f_{3dB-supercap}$	1 Hz
f_{sw}	20 kHz
f_{LPF}	1 Hz
f_{HPF}	5 Hz

TABLE I: Parameters for the simulations

chosen to show some remarkable voltage variation even with short simulation times. This condition emulates a request that cannot be satisfied by the fuel cells alone and where the energy storage system is required to provide the missing power. For simplicity, the battery and the fuel cell are modeled as ideal voltage sources, while resistors and controlled current sources simulate the loads at the bus. The QAB operates in voltage control mode, as described in Section IV. A voltage control bandwidth of 300 Hz is chosen for the bus regulator, while a very slow controller (1 Hz) was chosen for the supercapacitors. Choosing a slow controller ensures that there is not interaction between the other controls. Moreover, a voltage-dependent dynamic saturation of the phase shift of the supercapacitor port prevents its voltage to decrease or increase too much. In the case of saturation, the remaining power request is shifted from the supercapacitors to the batteries.

Fig. 11 shows a rapid change in the power consumption of the bus. The voltages and currents at each port are reported, as well as the phase shift. In Fig. 11a a current step of 10 A happens at t = 0.5 s. Since there is no feed-forward, the bandwidth of the controller determines the voltage restoration. Moreover, due to the slow dynamic, the supercapacitors are not providing the major share of the current, like it is expected. Fig. 11b shows the same transient with the feed-forward enabled. However, a static-gain decoupling is implemented. Differently from the previous case, the voltage regulation is improved, and almost no undervoltage appears. The currents show that the supercapacitors are supplying the current for the transient. Fig. 11c shows the effect of the dynamic decoupling. The effect of the dynamic decoupling is to modify the phase shift taking into account the voltage difference. Since it is expected that the supercapacitors will discharge, the phase shift is incremented to provide more power. In fact, a slightly deeper discharge of 2 V is visible. To sum up, for voltage difference up to 25 %, the static decoupling still allows excellent tracking performance.

Fig. 12 shows a ramp variation that happens at t = 0.7 s and ends at t = 1.2 s. In all cases, the supercapacitors are not involved in the power transfer. As can be seen from Fig. 12b and Fig. 12c, the decoupling has no effect on the performance, while the feed-forward allows for a slightly better regulation (0.2 V difference instead of 0.4 V) than in the case of Fig. 12a.

Fig. 13 shows the case where a high request from the load forces the QAB to operate at full power. It is expected that the supercapacitors will try to supply the power until the

This article has been accepted for publication in a future issue of this journal, but has not been fully edited. Content may change prior to final publication. Citation information: DOI 10.1109/TPEL.2017.2781258, IEEE Transactions on Power Electronics

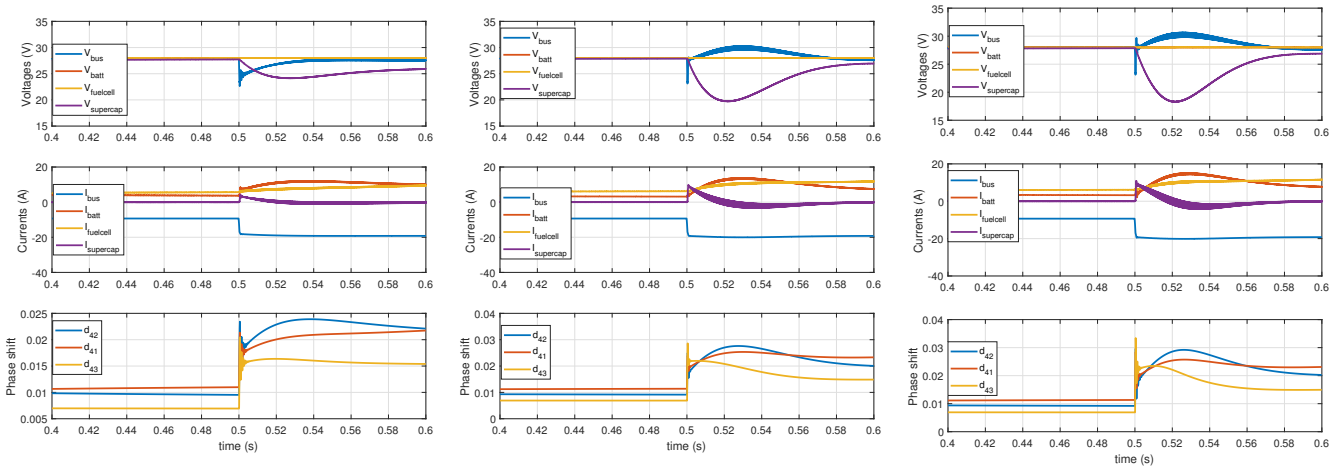

(a) Without current feed-forward and real-time decoupling

(b) With current feed-forward and with fixed decoupling.

(c) With current feed-forward and real-time decoupling

Fig. 11: Simulation results of the QAB with a load step and different control strategies.

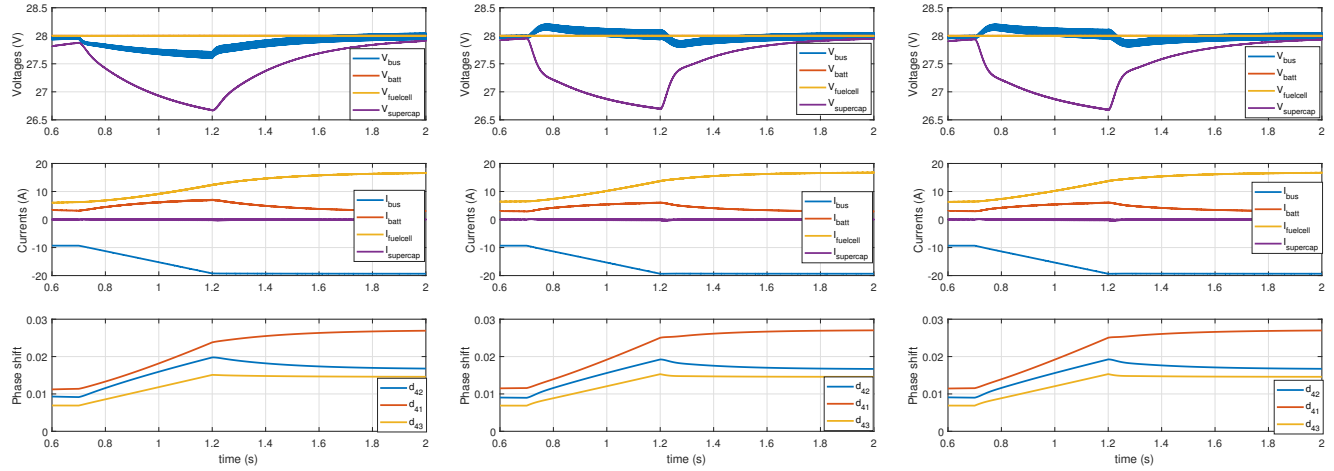

(a) Without current feed-forward and real-time decoupling

(b) With current feed-forward and with fixed decoupling.

(c) With current feed-forward and real-time decoupling.

Fig. 12: Simulation results of the QAB in case of a slow load variation.

voltage limit is reached. During these simulations, a maximum limit to 0.1 to the phase shift prior the decoupling is chosen. Considering the parameters chosen, this corresponds to a maximum current of 30 A. At time t = 0.5 s a triangular current demand up to 95 A is requested. As can be seen in Fig. 13a, without feed-forward there is a marked undervoltage and the supercapacitors are not supplying current because the variation is too slow. With the feed-forward, Fig. 13b the supercapacitors are correctly supplying the current, however the undervoltage is still present, because the voltage drop of the supercapacitor ports actually reduces the transfer ratio. Actually, with the chosen parameters, the undervoltage of Fig. 13b is compliant with the MIL-STD-704F (voltage greater than 18 V), while the one in Fig. 13a is not. The use of the static decoupling still represents an improvement. Fig. 13c shows the expected behavior, a minimum undervoltage appears, the supercapacitors are depleted to their limit, forcing also the batteries to provide peak power.

Finally, because reliability in aircraft application is of paramount importance, a simulation of a fault at the fuel cell port is presented. The simulated fault is a short circuit of a device, that forces the H-bridge connected to the fuel cell to shut down completely, interrupting the power. The fault detection can be realized with one of the many gate drivers that employ a desaturation protection. After disabling the gate drivers for the specified port, the control has to set the phase-shift of the fuel cell port to zero, shifting consequently the power request to the other ports. A further optimization would be to re-adapt the decoupling, considering that in the post-fault case, the converter operates as a triple active bridge (TAB),

This article has been accepted for publication in a future issue of this journal, but has not been fully edited. Content may change prior to final publication. Citation information: DOI 10.1109/TPEL.2017.2781258, IEEE Transactions on Power Electronics

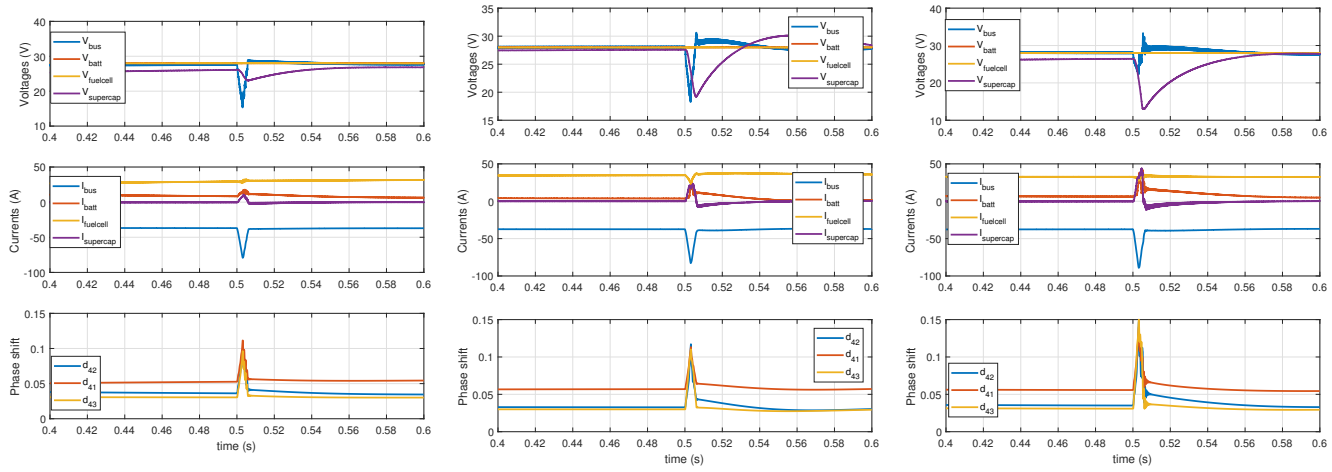

(a) Without current feed-forward and real-time decoupling.

(b) With current feed-forward and with fixed decoupling.

(c) With current feed-forward and real-time decoupling.

Fig. 13: Simulation results of the QAB during an overload condition, where all three energy sources must supply power.

with a consequent change of the inductance matrix. Although this would improve the decoupling, it will be shown in the simulation that is not necessary.

Fig. 14 shows the same case of Fig. 13, but at t = 0.504 (after the maximum power) the fuel cell is disconnected. As can be seen, the power is shifted at first to the supercapacitors, that discharge fast, then the battery takes care of providing the power. This condition can be sustained as long as the thermal design of the battery port allows for safe operations. In any case, the control is still stable. The oscillations are due to the change in the converter topology (and of the decoupling matrix), as mentioned before, but they do not challenge the system stability.

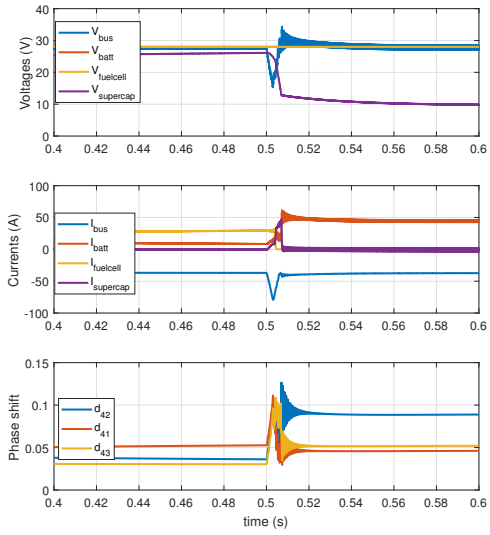

Fig. 14: Simulation results of a fault of the QAB at the fuel cell port.

VII. Experimental Results

The goal of the experiments is to show a demonstrator for the HV 270 V application, as well as to show that the proposed control allows to properly regulate the power transfer between different ports. The focus is to highlight that the asymmetric operation of the converter does not cause an excessive efficiency drop.

A prototype of the QAB was used to test the proposed control. SiC components (Wolfspeed C2M0025120D) were employed and a high efficiency has been demonstrated in previous publications [18]. High switching frequencies are desired for the dc-dc converter to increase the power density. Nevertheless, it results in higher di/dt and dv/dt ratios, and consequently in higher electromagnetic interference (EMI). Additionally, the high di/dt leads to voltage overshoots due to the parasitic inductance.

A high dv/dt implies higher efforts on the HF transformer, whose capacitive effects become more evident with the increasing voltage derivative. In fact, during the fast transient, the parasitic capacitance of the windings cause an uneven distribution of the voltage over each coils, increasing the probability of a partial discharge event. During partial discharge, current flows through the dielectric, causing losses, which in turn accelerate the dielectric deterioration. The dv/dt sets determines the probability of the partial discharge for the single commutation, while it was found that the partial discharge are actually proportional to the switching frequency [1]. For this reason, in order to safeguard the transformer health, a lower switching frequency can be advantageous. To avoid such problems, the switching frequency are usually selected in the range of 20 kHz to 100 kHz for MEA application [19]–[21]. The efficiency can also be optimized, when the selected switching frequency is this range.

For the HF transformer implementation, the shell type implementation was selected, where three E-shape cores (E80/38/20) from Epcos were used in parallel.

This article has been accepted for publication in a future issue of this journal, but has not been fully edited. Content may change prior to final publication. Citation information: DOI 10.1109/TPEL.2017.2781258, IEEE Transactions on Power Electronics

Considering the available equipment, the design is carried out at a reduced power, P_n = 3 kW. The nominal phase shift d_n = 0.1, leading to a needed inductance value of about 95 uH. As anticipated in the simulation results section, there is the degree of freedom to distribute the inductance between storage and bus ports, in this case a value of 160 uH was chosen for the storage ports and a smaller inductance (35 uH) was chosen for the bus port. Considering the leakage inductance of the transformer, the design value is reached. The transformer already showed asymmetries of 10 % of the leakage inductance because of the different winding of the bus port, so keeping the symmetry would not have brought any advantage. The devices are chosen for availability reasons and are overdesigned for the demonstrator. In particular, considering 270 V nominal voltage (with 350 maximum operating voltage considering the MIL-STD), devices with breakdown voltage of 650 V could have been chosen. However, SiC devices manufactured have invested resources in optimizing the 1.2 kV devices for market reasons, as a consequence devices with better characteristics in this voltage range can be found. Having devices with higher breakdown voltage rating could also benefit the cosmic rays immunity, especially important at higher altitudes. For this voltage range, also Si CoolMos devices (650 V) could be a valid alternative. Table II lists the parameters of the experimental results.

To sum up, the demonstrator and the experimental setup represent only partially the realistic flight conditions, where different optimizations would be carried out. However, the control principle is still valid and the efficiency difference in symmetrical/asymmetrical operation still holds qualitative validity despite the different parameters.

Fig. 15a shows a picture of the experimental setup, where the storage ports are connected to power supplies and the bus is emulated with electronic loads. It is assumed that all ports operate at the same DC voltage level for demonstration purpose. As a simplification, the decoupling is implemented with a constant matrix (the voltage variations are not taken into account).

Fig. 15 shows the results, in particular, Fig. 15b show the DC currents and the bus voltage in response to a load reduction. A load reduction was preferred instead of a load increase, because of unwanted transient due to the electronic loads during its turn-on. The port emulating the supercapacitors is providing the initial current peak, while the fuel cell shows a slow variation. This is in good agreement with the simulation of Fig. 11b: although the static decoupling is used, the performance is still very good.

V_n (V_1, V_2, V_3, V_4)	270 V
P_n	3 kW
L_1, L_2, L_3	160 uH
L_4	35 uH
L_{eq}	95 uH
C_1, C_2, C_3, C_4	0.4 mF
$f_{3dB-bus}$	100 Hz
f_{sw}	20 kHz

TABLE II: Experimental parameters

Fig. 15c shows the steady-state high-frequency waveforms for the QAB. As can be seen, the port emulating the fuel cell is providing the vast majority of the current, while the current of the other ports is reduced. The residual active power processed by the other ports (that should be zero in steady state) depends on the non-perfect compensation of the coupling. The outer voltage and SOC control would compensate for this effect in a real application.

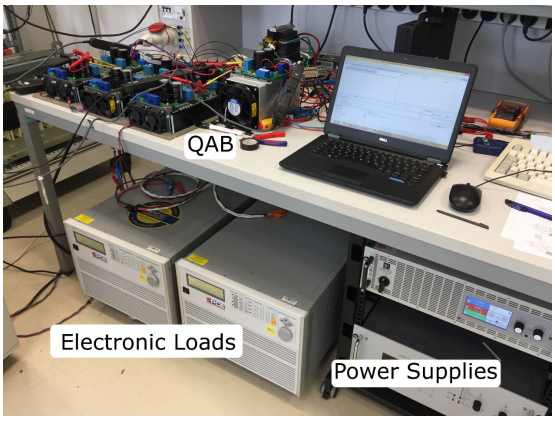

(a) Picture of the experimental setup.

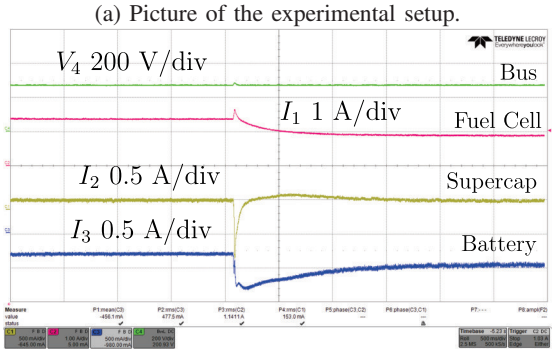

(b) Transient during load reduction.

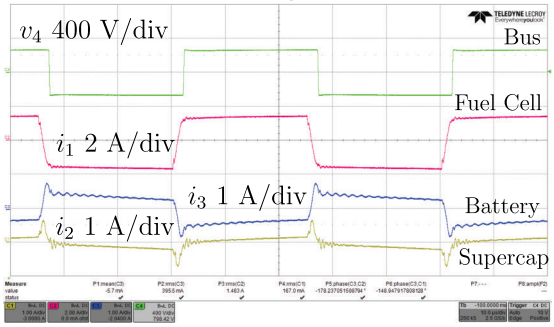

(c) Steady-state.

Fig. 15: Experimental results

The efficiency of the demonstrator was experimentally measured with the power meter Yokogawa WT1800. Two sets of measurements were performed: a first set where all three storage ports transfer power to the bus and a reduced set where only one storage port is transferring power to the bus. During this second test the other two storage ports are still switching and commutating with very low current. This represent the standard case where the fuel cell is providing the bulk power and the other storage are inactive. It also represents the most asymmetrical and challenging case, for this reason it was chosen to be measured. As can be seen, because of the

This article has been accepted for publication in a future issue of this journal, but has not been fully edited. Content may change prior to final publication. Citation information: DOI 10.1109/TPEL.2017.2781258, IEEE Transactions on Power Electronics

soft-switching operation as well as the reduced current that is flowing in the ports that are not transferring power, only a small efficiency deterioration of 0.1 % at 2 kW happens.

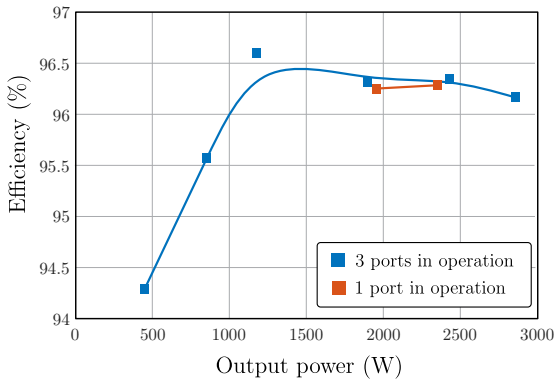

Fig. 16: Efficiency measurement of the QAB converter.

VIII. Conclusion

In this paper it has been demonstrated that the QAB converter can effectively be used as a storage manager for the More Electric Aircraft, guaranteeing the galavanic isolation between the ports and prioritizing the energy consumption from the fast energy sources. The main challenge is to control the power flow between different sources in a highly coupled structure of the QAB. The contribution of the paper is a novel decoupling control plus a feed forward action, that allows controlling the power flow regardless the controller bandwidth. Simulations show that in the case of small fast variations, the feed-forward is enough to guarantee good performance. As far as slow variations are concerned, neither feed-forward or dynamic decoupling are necessary. Both techniques are required to achieve optimal performance in the case of a peak power request that depletes the supercapacitor charge. Experiments carried out in a HV scenario shows that the converter can achieve a very good efficiency with the use of SiC devices and the efficiency deterioration due to asymmetrical operation is 0.1 % at 2 kW. This means that the QAB can effectively substitute three single-input single-output power converters for the storage integration.

Appendix I - QAB design formulas

$$P_n = V_n I_n \tag{4}$$

$$L_{eq} = \frac{V_n^2}{f_{sw} P_n} d_n \left(1 - 2|d_n|\right) \tag{5}$$

$$I_{L_{PK(bus)}} = \frac{V_n - \sqrt{V_n^2 - 8 L_{eq} f_{sw} V_n I_n}}{4 L_{eq} f_{sw}} \tag{6}$$

$$P_{MOS(cond)} = \frac{1}{T_{sw}} \int_0^{T_{sw}} R_{sd(on)}(i_{ds}, T_j, V_{gs}) i_{ds}^2 dt \tag{7}$$

$$P_{MOS(cond)} = R_{sd(on)} I_{S(rms)}^2 \tag{8}$$

$$P_{MOS(sw)} = \frac{1}{T_{sw}} \sum_{n=1}^{N_{sw(on)}} E_{on}(v_{ds}, i_{ds}, T_j, V_{gs}) + \frac{1}{T_{sw}} \sum_{n=1}^{N_{sw(off)}} E_{off}(v_{ds}, i_{ds}, T_j, V_{gs}) \tag{9}$$

$$P_{MOS(sw)} = \frac{1}{T_{sw}} \left(\sum_{n=1}^{N_{sw(off)}} E_{off}\left(I_d\right) \right) = E_{off} f_{sw} \tag{10}$$

$$I_{C_{0(rms)}} = \sqrt{I_{L_{PK(bus)}}^2 \left(1 - \frac{4d}{3}\right) - \left(\frac{V_n}{R_{load}}\right)^2} \tag{11}$$

$$P_{TR(wire)} = R_{wire} I_{TR(rms)}^2 \tag{12}$$

$$P_{core} = (\Delta B)^{\beta - \alpha} \frac{k_N}{T_{sw}} \int_0^{T_{sw}} \left|\frac{dB}{dt}\right|^{\alpha} dt \tag{13}$$

$$k_N = \frac{k}{(2\pi)^{\alpha-1} \int_0^{2\pi} |cos\theta|^{\alpha} d\theta} \tag{14}$$

Current	Coefficient	Current	Coefficient
$I_{L_{PK(storage)}}$	$\frac{1}{3}$	$I_{L_{rms(bus)}}$	$\sqrt{1 - \frac{4d}{3}}$
$I_{L_{rms(storage)}}$	$\frac{1}{3}\sqrt{1 - \frac{4d}{3}}$	$I_{D_{avg(storage)}}$	$\frac{d}{12}$
$I_{D_{rms(storage)}}$	$\frac{1}{3}\sqrt{\frac{d}{6}}$	$I_{S_{avg(storage)}}$	$\frac{1}{6}\left(1 - \frac{3d}{2}\right)$
$I_{S_{rms(storage)}}$	$\sqrt{\frac{1}{18}\left(1 - \frac{5d}{6}\right)}$	$I_{D_{avg(bus)}}$	$\frac{1}{2}\left(1 - \frac{3d}{2}\right)$
$I_{D_{rms(bus)}}$	$\sqrt{\frac{1}{2}\left(1 - \frac{5d}{6}\right)}$	$I_{S_{avg(bus)}}$	$\frac{d}{4}$
$I_{S_{rms(bus)}}$	$\sqrt{\frac{d}{6}}$		

TABLE III: Proportionality coefficients between semiconductor stress and peak inductor current $I_{L_{PK(bus)}}$.

IX. Acknowledgement

This work was supported by the European Research Council (ERC) under the European Unions Seventh Framework Program (FP/2007-2013)/ERC Grant Agreement 616344-HEART.

References

[1] D. Barater, G. Buticchi, A. Soldati, G. Franceschini, F. Immovilli, M. Galea, and C. Gerada, "Multistress characterization of insulation aging mechanisms in aerospace electric actuators," in *2015 IEEE Energy Conversion Congress and Exposition (ECCE)*, Sept 2015, pp. 2215–2222.

[2] P. Wheeler and S. Bozhko, "The more electric aircraft: Technology and challenges." *IEEE Electrification Magazine*, vol. 2, no. 4, pp. 6–12, Dec 2014.

[3] L. Rubino, D. Iannuzzi, G. Rubino, M. Coppola, and P. Marino, "Concept of energy management for advanced smart-grid power distribution system in aeronautical application," in *2016 International Conference on Electrical Systems for Aircraft, Railway, Ship Propulsion and Road Vehicles International Transportation Electrification Conference (ESARS-ITEC)*, Nov 2016, pp. 1–6.

[4] F. Gao, S. Bozhko, A. Costabeber, G. M. Asher, and P. W. Wheeler, "Control design and voltage stability analysis of a droop-controlled electrical power system for more electric aircraft," *IEEE Transactions on Industrial Electronics*, vol. PP, no. 99, pp. 1–1, 2017.

[5] A. Emadi, A. Khaligh, C. H. Rivetta, and G. A. Williamson, "Constant power loads and negative impedance instability in automotive systems: definition, modeling, stability, and control of power electronic converters and motor drives," *IEEE Transactions on Vehicular Technology*, vol. 55, no. 4, pp. 1112–1125, July 2006.

[6] X. Liu, A. J. Forsyth, and A. M. Cross, "Negative input-resistance compensator for a constant power load," *IEEE Transactions on Industrial Electronics*, vol. 54, no. 6, pp. 3188–3196, Dec 2007.

[7] M. Rashed, J. M. L. Peuvedic, and S. Bozhko, "Conceptual design of battery energy storage for aircraft hybrid propulsion system," in *2016 International Conference on Electrical Systems for Aircraft, Railway, Ship Propulsion and Road Vehicles International Transportation Electrification Conference (ESARS-ITEC)*, Nov 2016, pp. 1–6.

[8] S. Alahakoon and M. Leksell, "Emerging energy storage solutions for transportation a review: An insight into road, rail, sea and air transportation applications," in *2015 International Conference on Electrical Systems for Aircraft, Railway, Ship Propulsion and Road Vehicles (ESARS)*, March 2015, pp. 1–6.

[9] D. Salomonsson and A. Sannino, "Low-voltage dc distribution system for commercial power systems with sensitive electronic loads," *IEEE Transactions on Power Delivery*, vol. 22, no. 3, pp. 1620–1627, July 2007.

[10] H. Tao, A. Kotsopoulos, J. L. Duarte, and M. A. M. Hendrix, "Family of multiport bidirectional dc-dc converters," *IEE Proceedings - Electric Power Applications*, vol. 153, no. 3, pp. 451–458, May 2006.

[11] J. L. Duarte, M. Hendrix, and M. G. Simoes, "Three-port bidirectional converter for hybrid fuel cell systems," *IEEE Transactions on Power Electronics*, vol. 22, no. 2, pp. 480–487, March 2007.

[12] S. Falcones, R. Ayyanar, and X. Mao, "A dc-dc multiport-converter-based solid-state transformer integrating distributed generation and storage," *IEEE Transactions on Power Electronics*, vol. 28, no. 5, pp. 2192–2203, May 2013.

[13] R. Teodorescu, M. Liserre, and P. Rodriguez, *Grid Converters for Photovoltaic and Wind Power Systems*. Wiley, Jan 2011.

[14] L. Cao, K. H. Loo, and Y. M. Lai, "Output-impedance shaping of bidirectional dab dc-dc converter using double-proportional-integral feedback for near-ripple-free dc bus voltage regulation in renewable energy systems," *IEEE Transactions on Power Electronics*, vol. 31, no. 3, pp. 2187–2199, March 2016.

[15] M. K. Kazimierczuk, *High-Frequency Magnetic Components*. Wiley Publishing, 2009.

[16] K. Venkatachalam, C. R. Sullivan, T. Abdallah, and H. Tacca, "Accurate prediction of ferrite core loss with nonsinusoidal waveforms using only steinmetz parameters," in *Computers in Power Electronics, 2002. Proceedings. 2002 IEEE Workshop on*, June 2002, pp. 36–41.

[17] G. Buticchi, M. Andresen, M. Wutti, and M. Liserre, "Lifetime-based power routing of a quadruple active bridge dc/dc converter," *IEEE Transactions on Power Electronics*, vol. 32, no. 11, pp. 8892–8903, Nov 2017.

[18] G. Buticchi, L. Costa, and M. Liserre, "Improving system efficiency for the more electric aircraft: A look at dcdc converters for the avionic onboard dc microgrid," *IEEE Industrial Electronics Magazine*, vol. 11, no. 3, pp. 26–36, Sept 2017.

[19] M. Tariq, A. I. Maswood, C. J. Gajanayake, and A. K. Gupta, "Aircraft batteries: current trend towards more electric aircraft," *IET Electrical Systems in Transportation*, vol. 7, no. 2, pp. 93–103, 2017.

[20] S. Pugliese, R. A. Mastromauro, and S. Stasi, "270v/28v wide bandgap device-based dab converter for more-electric-aircrafts: Feasibility and optimization," in *2016 International Conference on Electrical Systems for Aircraft, Railway, Ship Propulsion and Road Vehicles International Transportation Electrification Conference (ESARS-ITEC)*, Nov 2016, pp. 1–6.

[21] B. Karanayil, M. Ciobotaru, and V. G. Agelidis, "Power flow management of isolated multiport converter for more electric aircraft," *IEEE Transactions on Power Electronics*, vol. 32, no. 7, pp. 5850–5861, July 2017.

Giampaolo Buticchi (S'10-M'13-SM'17) received the Masters degree in Electronic Engineering in 2009 and the Ph.D degree in Information Technologies in 2013 from the University of Parma, Italy. In 2012 he was visiting researcher at The University of Nottingham, UK. Between 2014 and 2017 he was a post-doctoral researcher at the University of Kiel, Germany. He is now Associate Professor in Electrical Engineering at The University of Nottingham Ningbo China. His research area is focused on power electronics for renewable energy systems, smart transformer fed micro-grids and dc grids for the More Electric Aircraft. He is author/co-author of more than 130 scientific papers.

Levy Ferreira Costa (S14) received the B.S. degree in electrical engineering from the Federal University of Ceara, Brazil, in 2010 and the M.S. degree from the Federal University of Santa Catarina, Brazil, in 2013. From 2013 to 2014, he was an Electrical Design Engineer with Schneider Electric, Brazil. He is currently working toward the Ph.D. degree at the Chair of Power Electronics, Christian-Albrechts-University of Kiel, Germany. His research interests include dc-dc converters, high-power converter systems and wide-bandgap semiconductors.

Davide Barater (S'11 - M'14) received the Masters degree in Electronic Engineering in 2009 and the Ph.D. degree in Information Technology in 2014 from the University of Parma Italy. He was an honorary scholar at the University of Nottingham, U.K., during 2012, and a visiting researcher at the University of Kiel, DE in 2015. He is currently working as research fellow at Department of Information Engineering, University of Parma, Italy. His research area is focused on power electronics for renewable energy systems and transport applications. He is author or coauthor of more than 45 international papers, published in scientific journals and conference proceedings, and holds one international patent.

Marco Liserre (S'00-M'02-SM'07-F13) received the MSc and PhD degree in Electrical Engineering from the Bari Polytechnic, respectively in 1998 and 2002. He has been Associate Professor at Bari Polytechnic and Professor at Aalborg University (Denmark). He is currently Full Professor and he holds the Chair of Power Electronics at Christian-Albrechts-University of Kiel (Germany). He has published over 300 technical papers (more than 86 of them in international peer-reviewed journals) and a book. These works have received more than 20000 citations. Marco Liserre is listed in ISI Thomson report The worlds most influential scientific minds.

Eugenio Dominguez Amarillo was born in 1976 and studied telecommunications engineering at the University of Seville. In 1999 he joined the TIC-109 Electronic Technology Group at that university, working as a researcher on industrial R+D projects. From 2005 to 2008 he was the managing director of the group's R+D laboratory, specializing in power electronics and renewable energy. He is the founding member of Win Inertia, and He is currently the managing director of a technological consultant brand GENTTECH, besides its functions as technological director and business development on power systems and energy storage for AEROSERTEC. His main research topics and his expertise are focused on power electronic topologies, control systems development and energy storage technologies. He is the author of seven patents focused on new applications and new concepts of energy storage technologies, and of 30 technical papers at conferences or in specialist national and international magazines.